Radiation Physics and Chemistry 198 (2022) 110274

Contents lists available at ScienceDirect

Radiation Physics and Chemistry

journal homepage: www.elsevier.com/locate/radphyschem

Real-time alpha-particle spectroscopy by a low-cost COTS digitizer system: A fast pulse-shaper incorporation

Hadi Kasani [a], Saleh Ashrafi [a,b,*], Nima Ghal-Eh [c]

[a] Faculty of Physics, University of Tabriz, P. O. Box 51666-16471, Tabriz, Iran
[b] Research Institute for Applied Physics and Astronomy, University of Tabriz, Tabriz, Iran
[c] Department of Physics, Faculty of Science, Ferdowsi University of Mashhad, P.O. Box 91775-1436, Mashhad, Iran

A R T I C L E I N F O

Keywords:
Alpha spectroscopy
PIN diode Detector
COTS digitizer
Pulse-shaper
Band-pass filter

A B S T R A C T

In this study, having designed the electronics readout and an appropriate PIN diode, the digital alpha-particle spectroscopy was undertaken by an external sound card digitizer. The designed electronic circuit simulation was performed using the LTSpice simulator. On the other hand, since the appropriate choice of digital pulse-shaper considerably improves the performance, a fast and easy-to-use pulse shaper was incorporated. A digital pulse-shaper based on a band-pass filter was also designed for the waveforms digitized by the sound card. The results of the energy resolution of the proposed pulse-shaper were compared with the results of conventional digital ones (i.e., trapezoidal, cusp-like, and FFT cusp-like). The results showed that band-pass filter-based pulse-shaper also improved the energy resolution as expected. The main advantages of the proposed pulse-shaper are its pulse-shaping speed (40% faster than the conventional ones) and ease of use (without needing to regulate parameters).

1. Introduction

Alpha particle spectroscopy has found many applications, especially in natural radioactivity measurements which require portable devices (Al-Masri and Blackburn, 1996; Percival and Martin, 1974). Solid-state detectors, such as surface-barrier, are suitable for the detection and spectroscopy of alpha particles. Commercial silicon photodiodes, such as PIN-diodes, are also being considered for detecting charged particles (Mangiarotti et al., 2021). With the advent of fast digitizers and powerful processors, the digital analyses of nuclear detector outputs are widely developed. Readily available digitizers, due to their both low-cost and simplicity have also been increasingly used in different applications (Kasani et al., 2021a, 2021b).

To achieve an optimized energy resolution, the use of appropriate pulse-shapers in digital spectroscopy with solid-state detectors is important. Different algorithms have been introduced and applied to shape the radiation detector output pulses. One of the most widely used algorithms for pulse-shaping is the digital trapezoidal pulse-shaper first developed by Jardanov et al. (Jordanov et al., 1994). Digital filters, on the other hand, can be used as pulse-shapers in the digital spectroscopy of charged particles.

The use of a sound card as a gamma-ray spectroscopy instrument was first introduced in the work of Sugihara et al. (2013), where it was used only as a digital MCA block. Whilst, in our previous paper (Kasani et al., 2021a), the sound card was utilized as a digitizer located just after the preamplifier for the gamma-ray spectroscopy by an NaI(Tl) scintillator. Note should be taken that the digital signal processing operations are different in NaI(Tl) scintillator and solid-state detectors, such that the pulse-shapers are used only in the latter (Nakhostin, 2017). In other words, the main difference in gamma-ray and alpha spectroscopy studies using a sound card is the detector type. Therefore, the first novelty of the present work is the operations of pulse-shapers on the signals digitized by the sound card.

In this study, having designed the pre-amplifier and amplifier circuits for a PIN diode detector, a digital alpha particle spectrometer has been constructed. The main advantage of the proposed system is that the time duration of the output pulses is such that can be acquired by inexpensive digitizers (e.g., a USB sound card). Furthermore, to achieve a suitable energy resolution and fast runtime, an appropriate pulse-shaper has been introduced in the pulse-shaper algorithm. Since the objective of this study is to propose a portable and inexpensive detector with simple operation useful in environmental radioactivity applications, the low count rate condition has been considered. The counting rate of 1 kcps and less is regarded as low in most references (e.g., in (Seino et al.,

* Corresponding author. Faculty of Physics, University of Tabriz, P. O. Box 51666-16471, Tabriz, Iran.
E-mail address: ashrafi@tabrizu.ac.ir (S. Ashrafi).

https://doi.org/10.1016/j.radphyschem.2022.110274
Received 8 December 2021; Received in revised form 19 April 2022; Accepted 28 May 2022
Available online 7 June 2022
0969-806X/

2012)). In this study, the count rate of 1 kcps is obtained by taking an average over the number of pulses in 150 waveforms with a duration of 1 s. Also, each DSP processor exhibits a dead time for signal processing, which depends on its RAM and the number of cores. Also, the spectroscopy results using the proposed shaper have been obtained without any pile-up rejection/correction and pole-zero cancellation.

Also, a pulse-shaper based on the band-pass filter with a 40% faster runtime than other conventional pulse-shapers has been presented. For most pulse-shapers, it is necessary to select the right regulatable parameters, which is sometimes a difficult task. However, the proposed pulse-shaper has the advantage that it does not require parameter adjustment.

2. Materials and methods

Here, the conventional digital algorithms which are used for shaping the radiation detector pulses are presented. Next, the results are compared with those obtained by the proposed algorithm in terms of ER and runtime data. The details of trapezoidal and finite flat-topped (FFT) cusp-like shapers have been discussed in (Ashrafi et al., 2020).

2.1. Digital algorithms

2.1.1. Proposed method: band-pass filter

A digital filter can be modeled as a linear time-invariant (LTI) system with constant coefficients. In the discrete-time domain, the input signal *x[n]*, and output signal *y[n]*are related by the following equation (Kuo et al., 2013),

$$y[n] = \sum_{k=-\infty}^{\infty} h[k]x[n-k] \tag{1}$$

where *h(k)* is the impulse response of the digital system which fully specifies the filter properties. The *z*-transform is a special form of the Laplace transform that converts an analog transfer function to a digital one, *H(z)*, in the digital domain. The output of the LTI system in the *z*-domain will be

$$Y(z) = H(z)\ \ X(z) \tag{2}$$

where *H(z)* is related to the impulse response of the digital system, *h[n]*, by the relation

$$H(z) = \sum_{-\infty}^{\infty} h[n]z^{-n}. \tag{3}$$

Hence, the transfer function for the IIR system may be written as

$$H(z) = \frac{Y(z)}{X(z)} = \frac{\sum_{k=0}^{M} b_k z^{-k}}{\sum_{k=0}^{N} a_k z^{-k}} \tag{4}$$

where b_k and a_k are a set of constant coefficients. This system is an example of a feedback system. The transfer function *H(z)* has the poles and zeroes in the *z*-plane which means the denominator and numerator of equation (4) equal zero in the *z*-plane. Here, the focus is on the filters with transfer function on the unit circle in the *z*-plane consisting of poles and zeros (Lynn, 1972). Since such poles may cause instability in the filter, they must be canceled by some zeros. The band-pass filters are obtained by placing the canceling pole(s) elsewhere on the unit circle. The design details of such filters are given in (Lynn, 1977). The transfer function of a second-order filter with 12 zeros on the unit circle and canceling poles at $\pm 60^\circ$ is given by

$$H(z) = \frac{(1 - z^{-12})^2}{(1 - z^{-1} + z^{-2})^2} \tag{5}$$

where the corresponding discrete-time domain recursive algorithm is

$$y(n) = 2y(n-1) - 3y(n-2) + 2y(n-3) - y(n-4) + x(n) - 2x(n-6) + x(n-12). \tag{6}$$

It is important to mention that the traditional pulse-shaping operation, described by Jordanove and Knoll (Jordanov and Knoll, 1994) is also a deconvolution of the transfer function for the analog amplifier and it can be substituted by an IIR digital filter. In this study, the band-pass filter is applied to the signals taken from a NaI(Tl) scintillation detector before and after a charge-sensitive preamplifier.

2.1.2. Cusp-like filter

The cusp-like shaping method is performed by the recursive difference equation in the time domain (Jordanov and Knoll, 1994). This algorithm converts an exponential pulse into a symmetrical-shaped pulse. First, parameter *M* is defined as $(\exp(1/\tau)-1)^{-1}$, where τ is the number of samples corresponding to the decay constant of the pulse. The following difference equations present the recursive model:

$$\begin{aligned} d^k(n) = v(n) - v(n-k),\ d^l(n) &= v(n) - v(n-1),\ p(n) \\ &= p(n-1) + d^k(n) - kd^l(n-1), n \geq 0,\ q(n) \\ &= q(n-1) + m_2 p(n), n \geq 0, s(n) \\ &= s(n-1) + q(n) + m_1 p(n), n \geq 0, \end{aligned} \tag{8}$$

where the v(n) is the input exponential signal, the s(n) is the output signal, m_2 is a parameter that determines the digital gain of the shaper, and $m_1 = m_2 M$.

2.2. Measurements

2.2.1. Detector design and construction

The detector (i.e., the PIN diode), the charge-sensitive preamplifier circuit, and the housing box are selected exactly as presented in (Ashrafi et al., 2020). Before digitizing the detector output using a USB sound card, an amplification stage is required. This was carried out by the commercial operational amplifier (Op-Amp). The full circuit map of the detector readout and a sample of the detector output pulse are shown in Figs. 1 and 3, respectively.

As shown in Fig. 1, PIN diode equivalent circuit includes a pulsed current source, shunt resistor, and detector capacitor .[1]

2.2.2. Digitizer system

A USB virtual 7.1 channel of an external sound card adapter (see Fig. 2) has been used for the data acquisition from detector output signals, which is based on a CM119 IC of a USB sound card. Since it easily plugs and plays with MS Windows, the extra drivers and power supply are omitted. This module digitizes the input signals with a sampling frequency of 192 kHz (i.e., 5.2 μs per sample), a resolution of 16 bits, and the nominal amplitude resolution of 0.03 mV. Furthermore, due to the presence of an attenuator in its input, it can digitize signals with even higher voltages.

The present study aims to use a sound card as a digitizer in such a way that the input circuit (i.e., anti-aliasing filter and attenuator) remains unchanged. To acquire real-time detector data, an 8th generation Corei5 Lenovo laptop (Intel Core i5-8265U CPU @ 1.60GHz-1.80 GHz) with 8 GB memory RAM has been used. Next, the data-acquisition toolbox of MATLAB software has been incorporated for the data acquisition, which can also provide a trigger for the data-acquisition procedure.

[1] https://tools.analog.com/en/photodiode/.

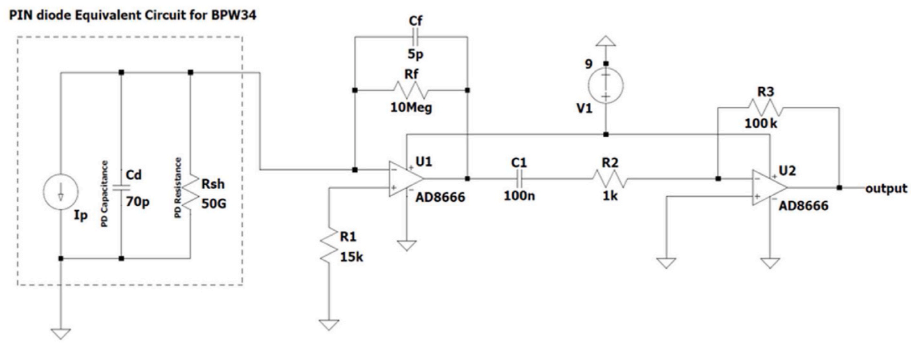

Fig. 1. Circuit diagram of the charge-sensitive pre-amplifier and amplifier stages of alpha particle spectrometer.

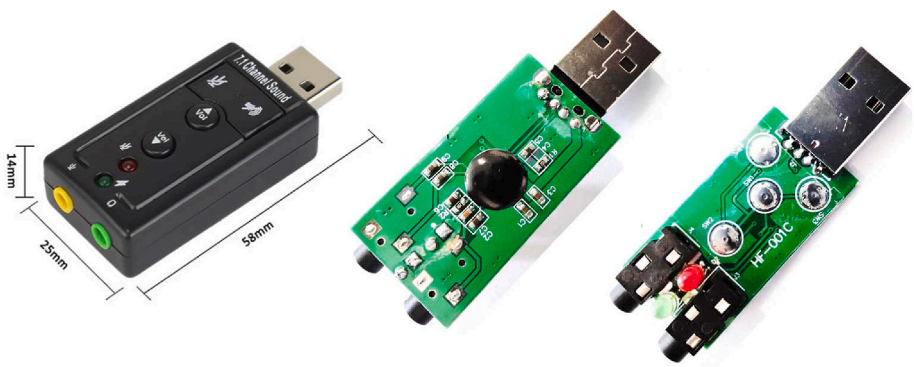

Fig. 2. The external USB sound card used in this study.

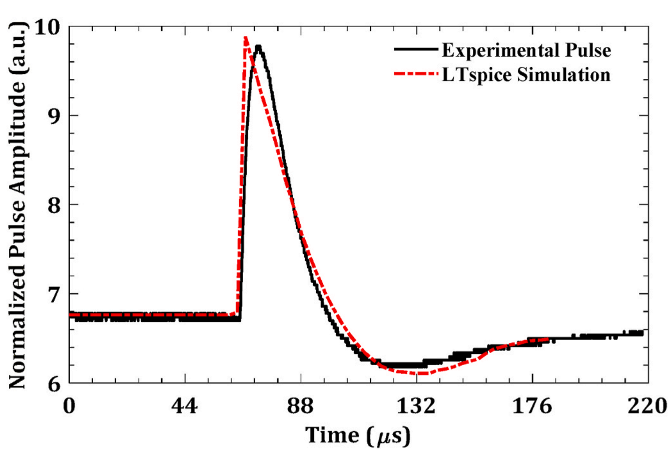

Fig. 3. Measured and LTSpice-simulated pulses of digital alpha-particle spectroscopy system.

3. Results and discussion

A sample pulse of the PIN detector output collected by a digital oscilloscope is shown in Fig. 3. The time length of Fig. 3 for this sample pulse (including 5000 samples) is 220 μs, or equivalently, each sample represents 44 ns. To compare the measured and LTSpice-simulated[2] pulses, the electronic circuit shown in Fig. 1 is used. The results are illustrated in Fig. 3.

To perform alpha-particle spectroscopy, the constructed detector is exposed to a 9 μCi ^{226}Ra source placed at an approximate distance of 1 cm. A full waveform length of 1s is chosen, and the pulse-shaping methods are implemented. First, to avoid sharp and nail-like peaks, the waveform is smoothed by a moving average (MA) filter with a window length of 5 samples Here, 100 free-pile-up pulses are selected from the smoothed waveform and their average is set as a sample pulse. As shown in Fig. 4 (left), the shape of the sample pulse is noticeably modified compared to the original one (Fig. 3), which is attributed to the input circuit of the USB sound card.

Since the input circuit of the sound card has to remain unchanged, the pulse-shapers are implemented on its digitized waveform. As can be seen in the specified region of Fig. 4, the lower and right part of the sample pulse exhibits a bi-exponential behavior, which is very similar to the output pulses of most radiation detectors. Therefore, in this work, the regulatable parameters of conventional pulse-shapers are selected according to Fig. 4 (right). The optimal parameter values in trapezoidal, cusp-like and FFT cusp-like filter methods of the present study are (k, M, l) = (7, 7.5, 1), (k, M, m_2) = (3, 7.5, 2) and (d, k, B) = (0.8, 4, 1), respectively.

Having implemented the MA filter and waveforms inversion, the pulse-shapers are utilized. In Fig. 5 (a), a part of the inversed measured waveform after applying the MA filter is illustrated, whilst, Fig. 5(b–e) show the same waveform when a band-pass (proposed method), trapezoidal, cusp-like, and FFT cusp-like filters are incorporated, respectively.

The pulse-shaping is implemented on the full waveform (with a length of 1 s) before the height of the digital pulse-shaper output is determined using the peak-detection algorithm of MATLAB. As it turns out, the pulse height is proportional to the energy of the incident particle to the detector.

To obtain the energy spectrum of alpha particles from ^{226}Ra source, the pulse heights are sorted and the energy calibration is carried out. Having sorted the pulse-height values, it can be seen that the count vs. channel plot has 4 separate peaks. However, the decay scheme of ^{226}Ra represents five energies (4.784, 5.0304, 5.489, 6.002, and 7.678 MeV) which are corresponding to ^{226}Ra, ^{210}Po, ^{222}Rn, ^{218}Po, and ^{214}Po,

[2] https://www.analog.com/en/design-center/design-tools-and-calculators/ltspice-simulator.html.

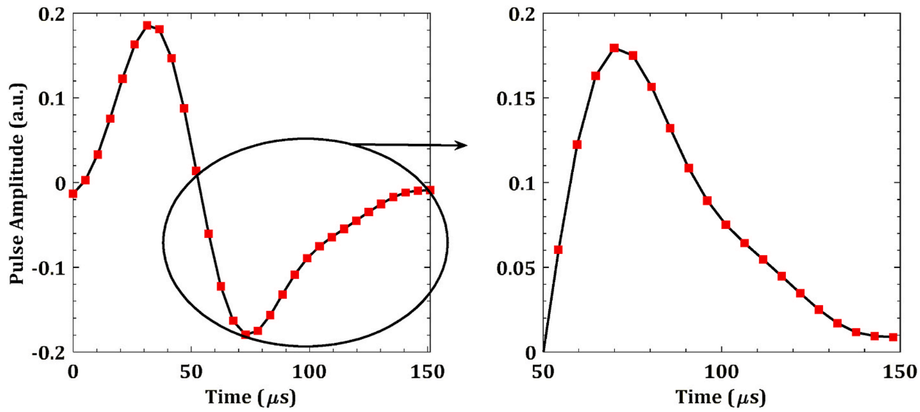

Fig. 4. Measured averaged sample pulse acquired using a USB sound card with a specified region of interest (left) and a reversed portion (right).

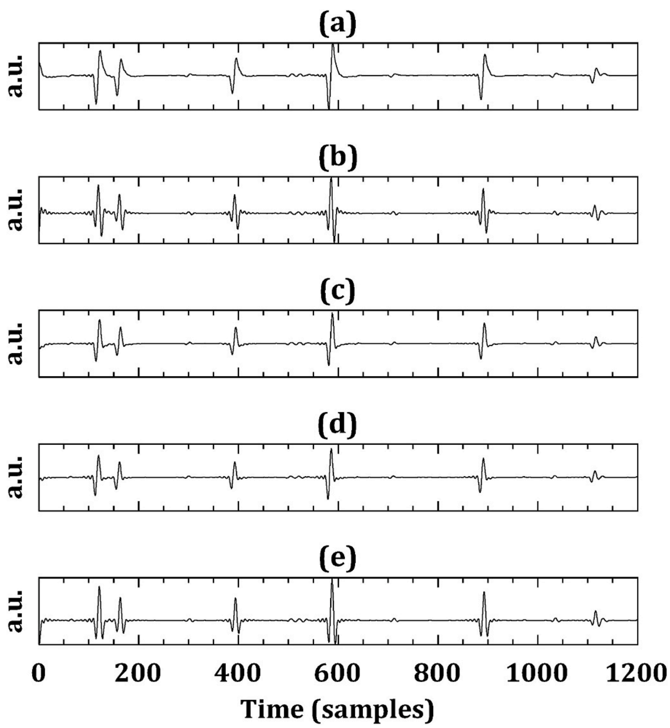

Fig. 5. (a) Digitized measured signals taken from a PIN-diode detector and the shaped ones using (b) band-pass (proposed), (c) trapezoidal, (d) cusp-like, and (e) FFT cusp-like methods.

respectively. But, the two 5.489 and 5.403 MeV energies are merged into a single peak and cannot be resolved by the detector of the present study.

The energy calibration is performed using the above energies and the corresponding channel numbers are assigned. Fig. 6 shows the energy spectra of the alpha particles measured when the detector without pulse-shaper is exposed to a ^{226}Ra. Since the baseline of the detector output waveforms is generally unstable due to parameters such as thermal drifts, detector leakage current, power-line disturbances, etc., the measurement of the pulse-height will have errors that prevent the peak location in the energy spectrum from being displayed correctly, especially at peaks of 4.78 MeV and 6.002 MeV. Because the pulse-shapers, to some extent, correct the baseline of the waveform which includes the output pulses of the detector, the above-mentioned error is slightly corrected (although a baseline restorer must be used after the pulse-shaper). Therefore, one may conclude that this difference is due to the instability of the baseline before using the pulse-shaper.

Using the multi-peak fit capability of Origin software, the full-width at half maximum (FWHM) values of the peaks and corresponding energy resolutions, ER (i.e., FWHM divided by peak energy) are calculated. The ER values for four different alpha particle energies of ^{226}Ra source, with and without the pulse shapers, are presented in Table 1.

The ER values show that for all alpha particle energies, except 7.69 MeV, the pulse-shaping has improved the ER. Also, the pulse-shaper with a band-pass filter (i.e., the proposed method) provides an acceptable result in improving ER as efficiently as conventional pulse-shapers. The improvement of energy resolution can be quantified by dividing the difference between the energy resolution, with and without using a

Table 1
Measured energy resolution (ER) using different digital shaping methods.

METHOD	ER@ 4.78 MeV (%)	ER @ 5.49 MeV (%)	ER @ 6.00 MeV (%)	ER @ 7.69 MeV (%)
Without shaper	12.9 ± 0.4	9.5 ± 0.2	6.5 ± 0.2	2.8 ± 0.0
Proposed method	11.3 ± 0.3	8.8 ± 0.2	6.1 ± 0.1	3.5 ± 0.0
Trapezoidal	12.1 ± 0.4	8.8 ± 0.3	5.7 ± 0.2	3.5 ± 0.0
Cusp-like	10.7 ± 0.4	8.5 ± 0.2	5.6 ± 0.2	3.5 ± 0.0
FFT cusp-like	10.7 ± 0.3	8.6 ± 0.2	5.7 ± 0.1	3.2 ± 0.0

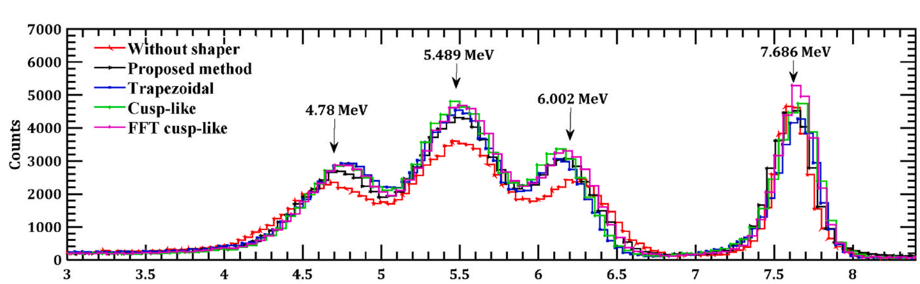

Fig. 6. Measured energy spectrum of the detector with and without pulse-shaper when exposed to ^{226}Ra alpha source.

pulse-shaper (See Table 1) by its value without a pulse-shaper. The improvements of energy resolution after applying pulse-shaper in the best case, at 4.784, 5.489, and 6.002 MeV, are 17, 10, and 13%, respectively.

The runtime of pulse-shaping algorithms is an important factor in real-time applications. In this study, the runtime for the trapezoidal, cusp-like, and FFT cusp-like filter methods are 0.15 ± 0.02 s, 0.15 ± 0.03 s, and 0.15 ± 0.03 s, respectively. Whilst, the runtime of the proposed algorithm (i.e., band-pass filter) is 0.09 ± 0.01 s, which exhibits a 40% improvement compared to conventional algorithms. Moreover, as mentioned earlier, the exclusion of regulatable parameters is an advantage of the proposed method. In our previous work (Ashrafi et al., 2020), a digital oscilloscope with an adjusted sampling rate of 2 MSPS was used. However, in this work, we had to use an amplifier unit due to the nature of the external audio card input. The results in some cases indicate the advantage of the sound card.

4. Conclusions

A low-cost digital alpha particle spectrometer was designed and constructed. The output pulse from the PIN detector stored by the digital oscilloscope was compared with the pulse simulated by LTSpice simulator software in terms of pulse shape. The digitization was carried out using a readily available USB sound card. By averaging over 100 pile-up-free pulses, a sample pulse was obtained through which the regulatable parameters of conventional pulse-shapers were selected. The results confirmed that using pulse-shapers, the energy resolution improved by 17%. To shape the pulses obtained from the sound card, a fast and easy-to-implement pulse-shaper was designed based on the band-pass filter, which resulted in an improvement in the runtime by 40%.

Author statement

The author's contributions to the submitted manuscript are as following:

Hadi Kasani: Writing, Conceptualization, Software, Data Curation, Testing.

Saleh Ashrafi: Conceptualization, Design, Methodology, Writing.

Nima Ghal-Eh: Investigation, Validation, Writing.

Declaration of competing interest

The authors declare that they have no known competing financial interests or personal relationships that could have appeared to influence the work reported in this paper.

Acknowledgments

The project has been supported by a research grant from the University of Tabriz (№ SAD/3/14000115).

References

Al-Masri, M., Blackburn, R., 1996. Radioanalytical methods for determination of alpha emitters in the environment. Radiat. Phys. Chem. 47, 171–175.

Ashrafi, S., Kasani, H., Ghal-Eh, N., Vega-Carrillo, H.R., 2020. Sparsity-based pulse-processor for digital α-particle spectroscopy with Si-PIN-Diode detector. Appl. Radiat. Isot. 163, 109245.

Jordanov, V.T., Knoll, G.F., 1994. Digital synthesis of pulse shapes in real time for high resolution radiation spectroscopy. Nucl. Instrum. Methods Phys. Res. Sect. A Accel. Spectrom. Detect. Assoc. Equip. 345, 337–345.

Jordanov, V.T., Knoll, G.F., Huber, A.C., Pantazis, J.A., 1994. Digital techniques for real-time pulse shaping in radiation measurements. Nucl. Instrum. Methods Phys. Res. Sect. A Accel. Spectrom. Detect. Assoc. Equip. 353, 261–264.

Kasani, H., Ashrafi, S., Ghal-Eh, N., 2021a. High count-rate digital gamma-ray spectroscopy using a low-cost COTS digitizer system. Radiat. Phys. Chem. 184, 109438.

Kasani, H., Ashrafi, S., Ghal-Eh, N., Vega-Carrillo, H.R., 2021b. Gamma-ray spectroscopy with anode pulses of NaI (Tl) detector using a low-cost digitizer system. Appl. Radiat. Isot., 109854

Kuo, S.M., Lee, B.H., Tian, W., 2013. Real-time Digital Signal Processing: Fundamentals, Implementations and Applications. John Wiley & Sons.

Lynn, P., 1972. Recursive digital filters with linear-phase characteristics. Comput. J. 15, 337–342.

Lynn, P., 1977. Online digital filters for biological signals: some fast designs for a small computer. Med. Biol. Eng. Comput. 15, 534–540.

Mangiarotti, A., Petri, A., Malafronte, A., Gonçalves, J., Barros, S., Bueno, C., Fernández-Varea, J., Maidana, N., Martins, M., Vanin, V., 2021. A low-cost small-size commercial PIN photodiode: II. Comparison of measurements with monoenergetic electrons to analytical expressions and Monte Carlo simulations. Radiat. Phys. Chem. 182, 109102.

Nakhostin, Mohammad, 2017. Signal Processing for Radiation Detectors. John Wiley & Sons.

Percival, D.R., Martin, D.B., 1974. Sequential determination of radium-226, radium-228, actinium-227, and thorium isotopes in environmental and process waste samples. Anal. Chem. 46, 1742–1749.

Seino, T., Takahashi, I., Ishitsu, T., Ueno, Y., Kobashi, K., 2012. An alternative pulse height correction method for pole zero cancellation circuitry. Nucl. Instrum. Methods Phys. Res. Sect. A Accel. Spectrom. Detect. Assoc. Equip. 675, 133–138.

Sugihara, K., Nakamura, S.N., Chiga, N., Fujii, Y., Tamura, H., 2013. Development of the low-cost multi-channel analyzer system for γ-ray spectroscopy with a PC sound card. Am. J. Phys. 81, 792–797.